From Incommensurate Correlations to Mesoscopic Spin Resonance in $YbRh_2Si_2$

C. Stock,[1,2] C. Broholm,[3,1] F. Demmel,[4] J. Van Duijn,[5] J. W. Taylor,[4] H. J. Kang,[1] R. Hu,[6] and C. Petrovic[6]

[1]*NIST Center for Neutron Research, 100 Bureau Drive, Gaithersburg, Maryland 20899, USA*
[2]*Indiana University, 2401 Milo B. Sampson Lane, Bloomington, Indiana 47404, USA*
[3]*Institute for Quantum Matter and Department of Physics and Astronomy, Johns Hopkins University, Baltimore, Maryland 21218, USA*
[4]*ISIS Facility, Rutherford Appleton Labs, Chilton, Didcot OX11 0QX, United Kingdom*
[5]*Instituto de Investigacin en Energas Renovables and Departamento de Fsica Aplicada, Universidad de Castilla-La Mancha, 02006 Albacete, Spain*
[6]*Condensed Matter Physics, Brookhaven National Laboratory, Upton, New York 11973, USA*

(Received 19 March 2012; published 17 September 2012)

Spin fluctuations are reported near the magnetic field—driven quantum critical point in $YbRh_2Si_2$. On cooling, ferromagnetic fluctuations evolve into incommensurate correlations located at $\mathbf{q_0} = \pm(\delta, \delta)$, with $\delta = 0.14 \pm 0.04$ r.l.u. At low temperatures, an in-plane magnetic field induces a sharp intradoublet resonant excitation at an energy $E_0 = g\mu_B\mu_0 H$ with $g = 3.8 \pm 0.2$. The intensity is localized at the zone center, indicating precession of spin density extending $\xi = 6 \pm 2$ Å beyond the $4f$ site.

DOI: 10.1103/PhysRevLett.109.127201 PACS numbers: 75.40.Gb, 74.70.Tx, 75.50.Cc

The development of intersite coherence among Kondo-screened ions is a phenomenon central to understanding the heavy fermion state and quantum phase transitions [1–4]. Here we use neutron scattering to monitor such correlations as a function of magnetic field and temperature in a clean system where disorder due to chemical substitution is not expected. These experiments show the formation of a coherent Kondo lattice and a low-temperature field driven transition to a dressed single ion phase.

$YbRh_2Si_2$ is a heavy fermion metal with weak antiferromagnetic order at very low temperatures ~50 mK [5]. The resistivity varies linearly with temperature ($\rho \sim T$), demonstrating a strong non-Fermi liquid character [6]. In a small magnetic field of ~0.7 T along the c axis (and ~0.06 T when the field is applied within the a-b plane), the magnetic order is suppressed and the non-Fermi liquid phase transformed continuously into a Landau Fermi liquid, where $\rho \sim T^2$ [7,8]. The change in Hall number and band structure calculations indicate a quantum critical transition in the electron density, which can be interpreted in terms of Fermi surface reconstruction or local quantum criticality [9–12]. At higher fields, de Haas–van Alphen measurements indicate a Lifshitz transition of the Fermi surface [13].

Despite the heavy fermion nature, electron-spin resonance (ESR) shows a signal indicative of localized Yb^{3+} $4f$ moment behavior under the application of field [14]. While some studies have been made on magnetic dynamics, little is known about the atomic scale magnetic correlations across the field-tuned quantum critical point [15,16].

In this Letter, we present a neutron inelastic scattering study of single crystalline $YbRh_2Si_2$. We will show that at zero field, the magnetic fluctuations are incommensurate. Under the application of a magnetic field, driving the system through the quantum critical point, commensurate underdamped fluctuations develop at the Zeeman energy of the Yb^{3+} $4f$ crystal field doublet. The momentum localized resonance, however, indicates a spin density that extends beyond the $4f$ ion.

Experiments on single crystalline $YbRh_2Si_2$ prepared using zinc flux were performed on the SPINS, and OSIRIS spectrometers and powder experiments (for a discussion, see Supplemental Material [17]) used MARI. Approximately 300 (with total mass ~3 g) single crystal samples (growth and characterization described in Ref. [18]) were coaligned in the (HHL) scattering plane using a similar method as described previously [19]. Experiments on SPINS used a focussing analyzer with 11° acceptance, $E_f = 3.7$ meV, and vertical magnetic fields up to 11 T. To probe the low-energy dynamics ($E < 0.5$ meV), we used the OSIRIS indirect spectrometer with $E_f = 1.84$ meV. The data on OSIRIS have been corrected for a background obtained by imposing detailed balance [20]. In both experiments, the temperature was monitored by a resistive thermometer attached near the sample. The lowest temperature achieved was 100 mK, so this experiment could not access the ordered state. Absolute normalization was performed against the (0, 0, 2) nuclear Bragg peak and through a comparison of the reported magnetic field dependent magnetization [21].

We first describe the magnetic fluctuations at low temperatures near the ordering transition. Figure 1 shows constant energy scans near the ferromagnetic $Q = (0, 0, 2)$ position at 100 mK. Panel (a) summarizes the OSIRIS and SPINS data, showing ridges extending along $\hbar\omega$. This demonstrates that the momentum dependence is controlled by a higher energy scale such as the Kondo temperature or the Fermi energy. As shown in the Supplemental Material [17], these incommensurate low-energy fluctuations are

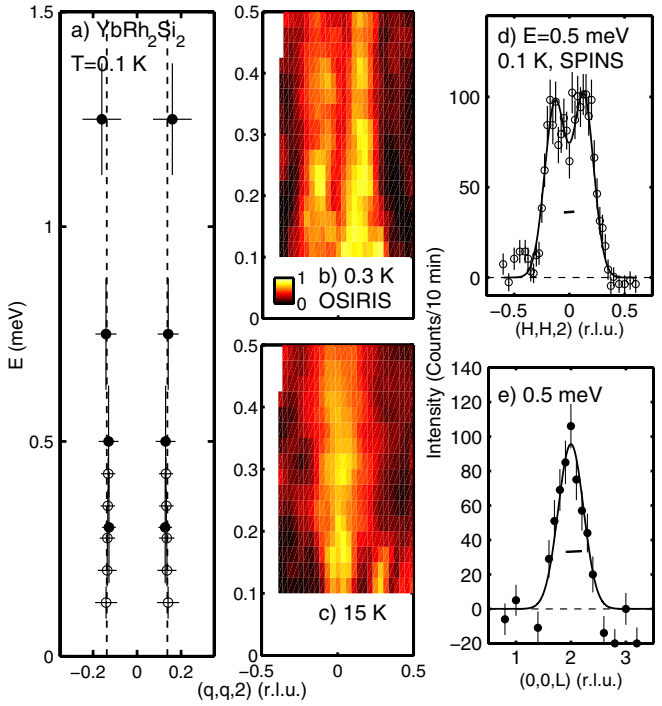

FIG. 1 (color online). The $\hbar\omega - Q$ dependence of the magnetic fluctuations in $YbRh_2Si_2$ at $T = 0.1$ K. (a) the position in Q of the ridges of scattering where filled (open) circles are from SPINS (OSIRIS). (b) and (c) plot the contour maps of the spin fluctuations taken on OSIRIS at 0.3 K and 15 K integrating over the range $(q, q, 2 \pm 0.25)$. (d) and (e) show the background-corrected cuts in momentum at 0.5 meV. The horizontal bars are the experimental resolution.

well below the first crystal field level located at 17.9 ± 0.6 meV and therefore are associated with allowed transitions within the ground-state doublet.

Panels (d) and (e) show representative scans taken on SPINS at 0.5 meV with a constant background subtracted. The scan along the $(H, H, 0)$ direction (d) illustrates an incommensurate modulation in the basal plane, while the scan along L [panel (e)] shows ferromagnetic interplane correlations. An $(H, H, 2 \pm 0.25)$-$\hbar\omega$ slice [panel (b)] demonstrates that the incommensurate ridges extend to the lowest energy transfers accessed (~ 0.1 meV). The fluctuations are peaked at $Q_\perp = (\delta, \delta)$ with $\delta = 0.14 \pm 0.4$, with no measurable dispersion or offset along L. We therefore expect (δ, δ) to be the characteristic wave vector of the low-temperature spin density wave order corresponding to the transition reported using muon spin relaxation (μSR) and susceptibility [5,6]. While there is no conclusive evidence that Fermi surface nesting drives this transition, the observed critical wave vector is not far from the spacing between large areas of the computed Fermi surface [11]. Low-temperature diffraction and calculations of $\chi(Q)$ will be required for progress.

At elevated temperatures of 15 K [panel (c)], the in-plane response changes considerably, with the incommensurate fluctuations being replaced by commensurate ferromagnetic excitations forming a ridge at the zone center. These results confirm a competition between ferromagnetic $q = 0$ excitations and incommensurate spin fluctuations, as inferred from NMR based on a comparison between the Knight shift and relaxation rate [22].

A more detailed survey of the T-dependent spin fluctuations can be found in Fig. 2. Constant $Q = (0, 0, 2)$ scans at 30 and 6.5 K are shown in panels (b) and (c). The solid curves are a fit to the relaxational form $\chi''(Q, \omega = \chi'_Q \omega \Gamma(T/[\Gamma(T^2 + \omega^2])))$, where $\Gamma(T)$ is the relaxation rate and χ'_Q the susceptibility. The temperature dependence of $\Gamma(T)$ [Fig. 2(a)] varies linearly and reaches zero close to $T = 0$. Such behavior is expected near quantum criticality.

In a similar manner to the case of scaling near a classical phase transition driven by thermal fluctuations, we investigate the scaling properties of the dynamic susceptibility

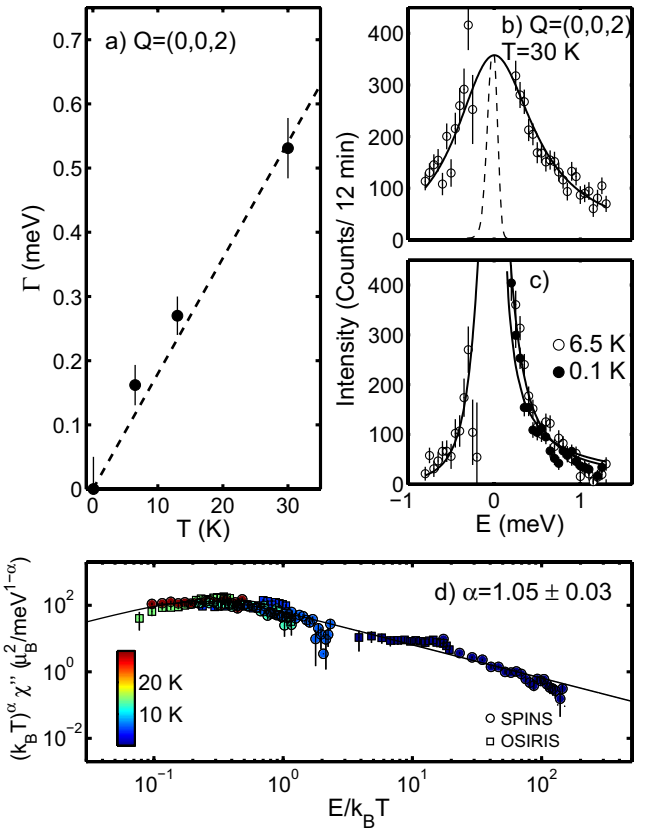

FIG. 2 (color online). (a) Illustration of the linewidth of the magnetic excitations taken from constant Q scans represented in panels (b) and (c) The dashed curve in (b) centered at $E = 0$ is the measured resolution on SPINS. Panel (d) summarizes all of the temperature dependence from SPINS and OSIRIS and plots $k_B T^\alpha \chi''$ as a function of $E/k_B T$ over the temperature range $T = [0.1, 30]$ K (as described by the color bar) and integrating over $Q = (\pm 0.1, \pm 0.1, 2 \pm 0.25)$ on OSIRIS. The exponent α was fitted to be $\alpha = 1.05 \pm 0.03$, as described in the Supplemental Material [17].

near the low-field quantum critical point. Several scaling theories have been proposed for the susceptibility [12,23]. The uniform dynamic susceptibility χ'' at all temperatures and energies from SPINS and OSIRIS are compiled in (d), which shows $(k_B T^{\alpha} \chi'')$ as a function of $E/k_B T$. The data are best fit with $\alpha = 1.05 \pm 0.03$ consistent with 1, as expected in the case of an itinerant ferromagnetic at $T > T_{\mathrm{Curie}}$ and $\Gamma \propto 1/\chi'_{\mathbf{q}}$, when $\chi'_{\mathbf{q}}$ has a Curie form [24]. The exponent is the same as observed for the scaling of heat capacity [6]. Such a scenario is consistent with the fluctuations being close to ferromagnetic, as reported in Fig. 1, and are similar to the case of UCoGe, which is close to a critical point between ferromagnetism and superconductivity [25].

We now investigate the possibility of anomalous scaling in our experiment, which would manifest as a deviation from the conventional scaling described above [23]. A fit to $k_B T^{\beta} \chi''$ as a function of $E/(k_B T^{\beta})$ resulted in $\beta = 0.92 \pm 0.05$, also consistent with 1 but different from other scenarios used to describe the fluctuations in $CeCu_2Si_2$ and $CeCu_{6-x}Au_x$ where such an analysis gave $\beta = 1.5$ [26]. The critical dynamics in $CeCu_{6-x}Au_x$ was also found to be described with $\alpha = 0.75$ (Ref. [27]), also different from $YbRh_2Si_2$. While anomalous scaling may exist close to the quantum critical point, our data at $Q \sim 0$ do not require such forms. Indeed, the scaling exponent we derive indicates that we are in the quantum disordered regime and higher resolution measurements at fields, temperatures, and wave vectors closer to the critical point are required to make contact with the anomalous thermodynamic data.

Next, we study the low temperature incommensurate fluctuations as a function of field. The result is summarized in Fig. 3 for an $[1\bar{1}0]$ field where the critical field is $\sim$0.06 T. Figure 3(a) illustrates that at 5 T a spin resonance develops, with the solid line a fit to an underdamped simple harmonic oscillator plus a relaxational form to describe the low-energy dynamics. Figures 3(b) and 3(c) plot constant energy scans at the resonance energy (1.05 meV) and below at 0.5 meV. The resonance is found to be localized in Q space, with the fluctuations below the resonance retaining the incommensurate structure measured at zero field. The solid curve in Fig. 3(b) is a resolution convolved fit to a Lorentzian squared resulting in a dynamic correlation length of $\xi = 6 \pm 2$ Å. This indicates that the resonance involves a finite region of correlated spins. Figure 3(d) illustrates a contour plot taken on OSIRIS at 1.25 T, demonstrating that the resonance peak (even at small magnetic fields) is localized in energy and momentum. Searches for dispersing spin excitations located in q away from the resonance peak, as measured in ferromagnetic MnSi (Ref. [28]) and calcium ruthenate (Ref. [29]) under an applied magnetic field in the paramagnetic state, failed to observe any dispersing modes. Therefore, the resonance peak measured here is not indicative of field-induced spin waves, like in other itinerant ferromagnets, but rather

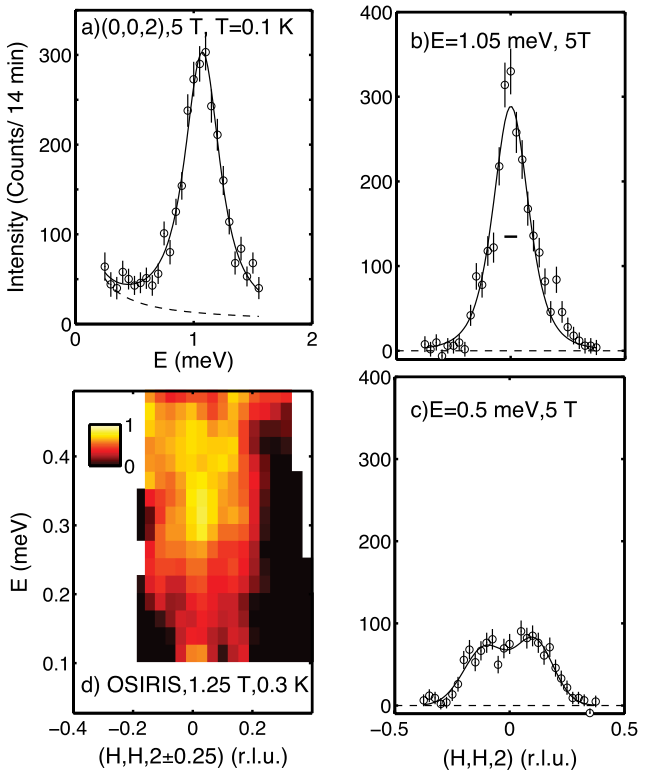

FIG. 3 (color online). (a) Background-subtracted constant Q scan acquired on SPINS showing a sharp magnetic resonance peak in a 5 T field. (b) and (c) show constant energy scans at (1.05 meV) and below (0.5 meV) the resonance energy. (d) color image of neutron scattering intensity data taken on OSIRIS, showing that the resonance peak in a field of 1.25 T is peaked in momentum and energy transfer.

represents a coherent precession of spin density extending beyond a $4f$ site.

The magnetic field dependence of the resonance peak displayed in Fig. 4(a) shows that the resonance energy varies as $g\mu_B\mu_0 H$ with $g = 3.8 \pm 0.2$ and remains underdamped at all measured fields, with little change in the linewidth. Background-corrected constant Q scans tracking the resonance with field are shown in panels (c)–(e). The integrated weight is also field independent, as shown in panel (b), and matches the calculated spectral weight for intradoublet transitions (or transverse fluctuations) (see Supplemental Material [17]). Therefore, all of the Yb^{3+} ions are contributing. The g factor is comparable to 3.6 obtained from ESR (Ref. [30]) and is consistent with the crystal field scheme described in Supplemental Material [17]. Therefore, the ESR signal and the neutron scattering resonance have a common origin and are both associated with the field-split ground-state doublet of the Yb^{3+} ions.

The presence of both a sharp magnetic field–induced resonance and an ESR signal are unique to $YbRh_2Si_2$ among heavy fermion materials. In heavy electron systems, an ESR signal is typically observed only in the presence of local Kondo impurities. At the phemenological

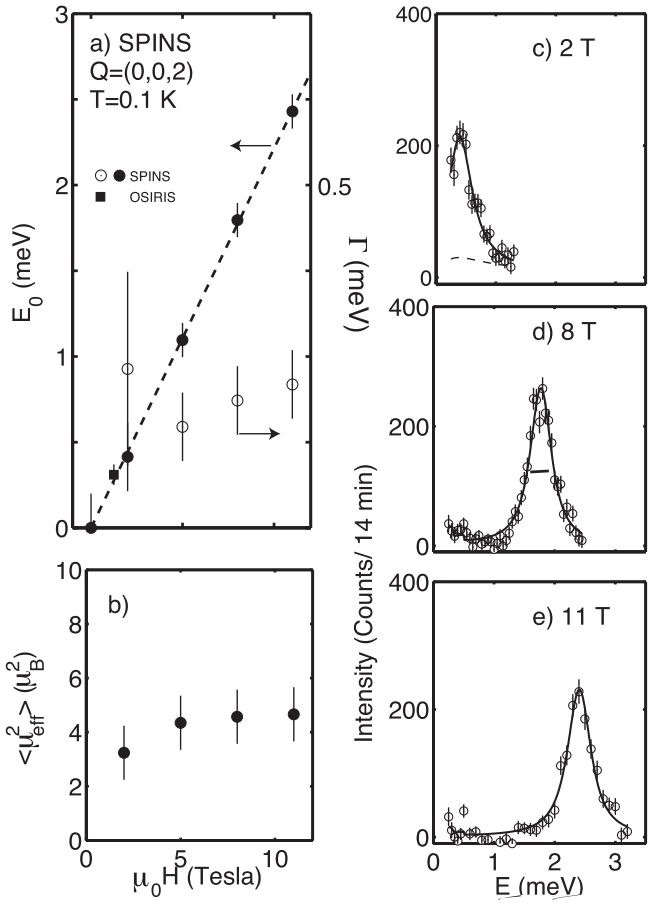

FIG. 4. (a) Illustration of the magnetic field dependence of the resonance energy and linewidth; (b) shows the integrated intensity in absolute units. Representative constant Q scans are shown in panels (c)–(e) at various magnetic fields.

level, the neutron experimental result is similar to the Haldane spin chain $Y_2BaNi_{1-x}Mg_xO_5$ with Mg impurities [31]. In that system, a magnetic field was found to induce a resonance peak, which is sharp in energy and momentum, representing a staggered magnetization near the edge of a Haldane chain segment. The finite linewidth in momentum was associated with a dynamic correlation length measuring the extent of the impurity edge state. Similar arguments have been applied to low-energy resonant field–induced effects in underdoped cuprates, possibly the result of exciting free spins near charge-rich regions [32].

A similar physical picture may be applied to $YbRh_2Si_2$. A magnetic field induces localized droplets of Yb^{3+} spins, which can be resonantly excited through intradoublet transitions. The localized region of spins are analogous to a Kondo impurity, which would give rise to an ESR signal. The length scale for such a Kondo impurity spin should be related to $\xi \sim \hbar v_f/k_B T_{\mathrm{Kondo}} = \hbar^2 k_f/m k_B T_{\mathrm{Kondo}}$ [33]. Taking $T_{\mathrm{Kondo}} = 24$ K, $k_f \sim 0.5a^*$, and $\gamma \sim 1.5$ J/mol K^2 (Ref. [6] at 0.1 K at zero field) yields a length scale of $\sim$15 Å. The result is on the same order as the dynamic correlation length of 6 Å extracted above, indicating that ξ may be set by the Kondo temperature and Fermi velocity. Because the effect is not due to purely localized Yb^{3+} ions, and is not associated with correlated dynamics over long length scales, we refer to this resonance as mesoscopic. The lack of Fermi surface nesting at high fields, the large Fermi velocity, and the heavy nature of the bands appear to result in the formation of Kondo screened ions. Such effects appear to be supported by ferromagnetic fluctuations, and similar results may exist in other ferromagnetic heavy fermion metals as well [34–36].

Our experiments indicate that the low-temperature zero field dynamics of $YbRh_2Si_2$ is effected by Fermi surface nesting, while at high fields and temperatures the response mimics Kondo-screened spins above a ferromagnetic transition.

We acknowledge funding from the STFC and the NSF through DMR-0116585 and DMR-0944772. Work at IQM was supported by DoE, Office of Basic Energy Sciences, Division of Materials Sciences and Engineering, under Award DE-FG02-08ER46544. Part of this work was carried out at the Brookhaven National Laboratory, which is operated for the U.S. Department of Energy by Brookhaven Science Associates (DE-Ac02-98CH10886) (R. H. and C. P.). We thank J. Murray and Z. Tesanovic for discussions and R. Down and E. Fitzgerald for cryogenic support.

[1] J. A. Hertz, Phys. Rev. B **14**, 1165 (1976).
[2] P. Gegenwart, Q. Si, and F. Steglich, Nature Phys. **4**, 186 (2008).
[3] H. V. Löhneysen and P. Wölfle, Rev. Mod. Phys. **79**, 1015 (2007).
[4] S. Ernst, S. Kirchner, C. Krellner, C. Geibel, G. Zwicknagl, F. Steglich, and S. Wirth, Nature (London) **474**, 362 (2011).
[5] K. Ishida, D. E. MacLaughlin, B. L. Young, K. Okamoto, Y. Kawasaki, Y. Kitaoka, G. J. Nieuwenhuys, R. H. Heffner, O. O. Bernal, W. Higemoto, A. Koda, R. Kadono, O. Trovarelli, C. Geibel, and F. Steglich, Phys. Rev. B **68**, 184401 (2003).
[6] O. Trovarelli, C. Geibel, S. Mederle, C. Langhammer, F. M. Grosche, P. Gegenwart, M. Lang, G. Sparn, and F. Steglich, Phys. Rev. Lett. **85**, 626 (2000).
[7] P. Gegenwart, J. Custers, C. Geibel, K. Neumaier, T. Tayama, K. Tenya, O. Trovarelli, and F. Steglich, Phys. Rev. Lett. **89**, 056402 (2002).
[8] J. Custers, P. Gegenwart, H. Willhelm, K. Neumaler, Y. Tokiwa, O. Trovarelli, C. Geibel, F. Steglich, C. Pepin, and P. Coleman, Nature (London) **424**, 524 (2003).
[9] S. Paschen, T. Luhmann, S. Wirth, P. Gegenwart, O. Trovarelli, C. Geibel, F. Steglich, P. Coleman, and Q. Si, Nature (London) **432**, 881 (2004).
[10] S. Friedemann, N. Oeschler, S. Wirth, C. Krellner, C. Geibel, F. Steglich, S. Paschen, S. Kircher, and Q. Si, Proc. Natl. Acad. Sci. U.S.A. **107**, 14547 (2010).

[11] M. R. Norman, Phys. Rev. B **71**, 220405(R) (2005).
[12] Q. Si, S. Rabello, K. Ingersent, and J. L. Smith, Nature (London) **413**, 804 (2001).
[13] P. M. C. Rourke, A. McCollam, G. Lapertot, G. Knebel, J. Flouquet, and S. R. Julian, Phys. Rev. Lett. **101**, 237205 (2008).
[14] J. Sichelschmidt, V. A. Ivanshin, J. Ferstl, C. Geibel, and F. Steglich, Phys. Rev. Lett. **91**, 156401 (2003).
[15] O. Stockert, M. Koza, J. Ferstl, A. Murani, C. Geibel, and F. Steglich, Physica (Amsterdam) **378B**, 157 (2006).
[16] O. Stockert, M. Koza, J. Ferstl, C. Geibel, and F. Steglich, Sci. Tech. Adv. Mater. **8**, 371 (2007).
[17] See Supplemental Material at http://link.aps.org/supplemental/10.1103/PhysRevLett.109.127201 for information about the experimental setup and sample, a description of the crystal field level scheme for Yb^{3+} in $YbRh_2Si_2$, and a more detailed analysis of the scaling properties.
[18] R. Hu, J. Hudis, C. Stock, C. Broholm, and C. Petrovic, J. Cryst. Growth **304**, 114 (2007).
[19] C. Stock, C. Broholm, J. Hudis, H. J. Kang, and C. Petrovic, Phys. Rev. Lett. **100**, 087001 (2008).
[20] T. Hong, M. Kenzelmann, M. M. Turnbull, C. P. Landee, B. D. Lewis, K. P. Schmidt, G. S. Uhrig, Y. Qiu, C. Broholm, and D. Reich, Phys. Rev. B **74**, 094434 (2006).
[21] P. Gegenwart, Y. Tokwa, T. Westerkamp, F. Weichert, J. Custers, J. Ferstl, C. Krellner, C. Geibel, P. Kerschl, K.-H. Huller, and F. Steglich, New J. Phys. **8**, 171 (2006).
[22] K. Ishida, K. Okamoto, Y. Kawasaki, Y. Kitaoka, O. Trovarelli, C. Geibel, and F. Steglich, Phys. Rev. Lett. **89**, 107202 (2002).
[23] A. J. Millis, Phys. Rev. B **48**, 7183 (1993).
[24] T. Moriya, J. Magn. Magn. Mater. **14**, 1 (1979).
[25] C. Stock, D. A. Sokolov, P. Bourges, P. H. Tobash, K. Gofryk, F. Ronning, E. D. Bauer, K. C. Rule, and A. D. Huxley, Phys. Rev. Lett. **107**, 187202 (2011).
[26] O. Stockert, M. Enderle, and M. v. Lohneysen, Phys. Rev. Lett. **99**, 237203 (2007).
[27] A. Schröder, G. Aeppli, R. Coldea, M. Adams, O. Stockert, H. v. Löhneysen, E. Bucher, R. Ramazashvili, and P. Coleman, Nature (London) **407**, 351 (2000).
[28] Y. Ishikawa, G. Shirane, J. A. Tarvin, and M. Kohgi, Phys. Rev. B **16**, 4956 (1977).
[29] P. Steffens, O. Friedt, Y. Sidis, P. Link, J. Kulda, K. Schmalzl, S. Nakatsuji, and M. Braden, Phys. Rev. B **83**, 054429 (2011).
[30] J. G. S. Duque, E. M. Bittar, C. Adriano, C. Giles, L. M. Holanda, R. Lora-Serrano, P. G. Pagliuso, C. Rettori, C. A. Perez, R. Hu, C. Petrovic, S. Maquilon, Z. Fisk, D. L. Huber, and S. B. Oseroff, Phys. Rev. B **79**, 035122 (2009).
[31] M. Kenzelmann, G. Xu, I. A. Zaliznyak, C. Broholm, J. F. DiTusa, G. Aeppli, T. Ito, K. Oka, and H. Takagi, Phys. Rev. Lett. **90**, 087202 (2003).
[32] C. Stock, W. J. L. Buyers, K. C. Rule, J. H. Chung, R. Liang, D. Bonn, and W. N. Hardy, Phys. Rev. B **79**, 184514 (2009).
[33] I. Affleck and P. Simon, Phys. Rev. Lett. **86**, 2854 (2001).
[34] E. Abrahams and P. Wolfle, Phys. Rev. B **78**, 104423 (2008).
[35] C. Krellner, T. Forster, H. Jeevan, C. Geibel, and J. Sichelschmidt, Phys. Rev. Lett. **100**, 066401 (2008).
[36] B. I. Kochelaev, S. I. Belov, A. M. Skvortsova, A. S. Kutuzov, J. Sichelschmidt, J. Wykhoff, C. Geibel, and F. Steglich, Eur. Phys. J. B **72**, 485 (2009).